Finite Element Predictions for the Thermoelastic Properties and Interphase Fracture of Titanium Nitride /AA3003 Alloy Particle-Reinforced Composites

[1]P. M. Jebaraj and A. Chennakesava Reddy[2]

[1]Professor, Department of Mechanical Engineering, Dr. Ambedkar Institute of Technology, Bangalore, India.
[2]Associate Professor, Department of Mechanical Engineering, Vasavi College of Engineering, Hyderabad, India
dr_acreddy@yahoo.com

Abstract: *In the present work, the AA3003/TiN metal matrix composites were manufactured at 10% and 30% volume fractions of TiN. The composites were subjected to mechanical and thermal loads. The microstructure of AA3003 alloy/TiN reveals the fracture of interphase and TiN particle.*

Keywords: *AA3003, titanium nitride, spherical nanoparticle, RVE model, finite element analysis, interphase fracture.*

1. INTRODUCTION

Thermo-elastic composites constitute an important class of materials with a wide variety of applications ranging from aerospace structures and electronic printed circuit boards to recreational and commercial equipment. Some of the most important and useful properties of these composites are lightweight, high strength and stiffness, excellent frictional properties, good resistance to fatigue and retention of these properties at high temperatures. Many authors have developed techniques to study the elastic behavior of particulate composites. They take into account the existence of an intermediate layer between the matrix and the particle [1]. These thin layers are called interphases or interfacial zones between particle and matrix. Although small in thickness, interphases can significantly affect the overall mechanical properties of the particle-reinforced composites. It is the weakest link in the load path, and consequently most failures in particle reinforced composites, such as debonding and matrix cracking, occur in or near this region. Thus, it is crucial to understand the mechanism and effects of the interphases on the overall material properties of fiber reinforced composites. Several homogenization techniques have been developed to obtain a suitable constitutive model to be inserted at the macroscopic level [2-17]. The macroscopic properties are determined by a homogenization process, which yields the effective stresses and strains acting on the effective, homogenized sample of material. The sample of material is often called as statistically representative volume element (RVE) or unit cell [18].

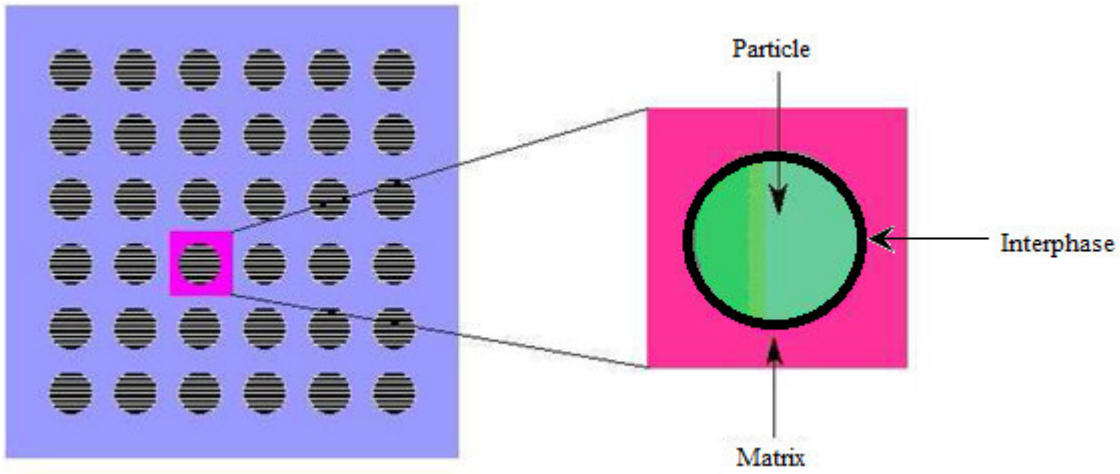

Figure 1: The interphase in a nanoparticle-reinforced composite.

Titanium nitride (TiN) oxidizes at 800 °C at normal atmosphere. It is chemically stable at room temperature and is attacked by hot concentrated acids. A well-known use for TiN coating is for edge retention and corrosion resistance on machine tooling, such as drill bits and milling cutters, often improving their lifetime by a factor of three or more. s a coating it is used

in aerospace and military applications and to protect the sliding surfaces of suspension forks of bicycles and motorcycles as well as the shock shafts of radio controlled cars. Due to their high biostability, TiN layers may also be used as electrodes in bioelectronic applications like in intelligent implants or in-vivo biosensors that have to withstand the severe corrosion caused by the body fluid. In the current work, the effect of temperature on the fracture in AA3003 alloy/TiN composites was examined. The shape TiN nanoparticle considered in this work is spherical. The periodic particle distribution was a square array as shown in figure 1. Both microscopic and micromechanics methods were employed to assess fracture in the composites.

2. MATERIALS METHODS

The matrix material was AA3003 alloy. The reinforcement material was TiN nanoparticles of average size 100nm (figure 2). The mechanical properties of materials used in the present work are given in table 1.

Table 1: Mechanical properties of AA3003 matrix and TiN nanoparticles

Property	AA3003	TiN
Density, g/cc	2.73	5.22
Elastic modulus, GPa	68.9	251.0
Coefficient of thermal expansion, 10^{-6} 1/^{o}C	21.08	9.35
Specific heat capacity, J/kg/^{o}C	893	757
Thermal conductivity, W/m/^{o}C	163	19.2
Poisson's ratio	0.33	0.25

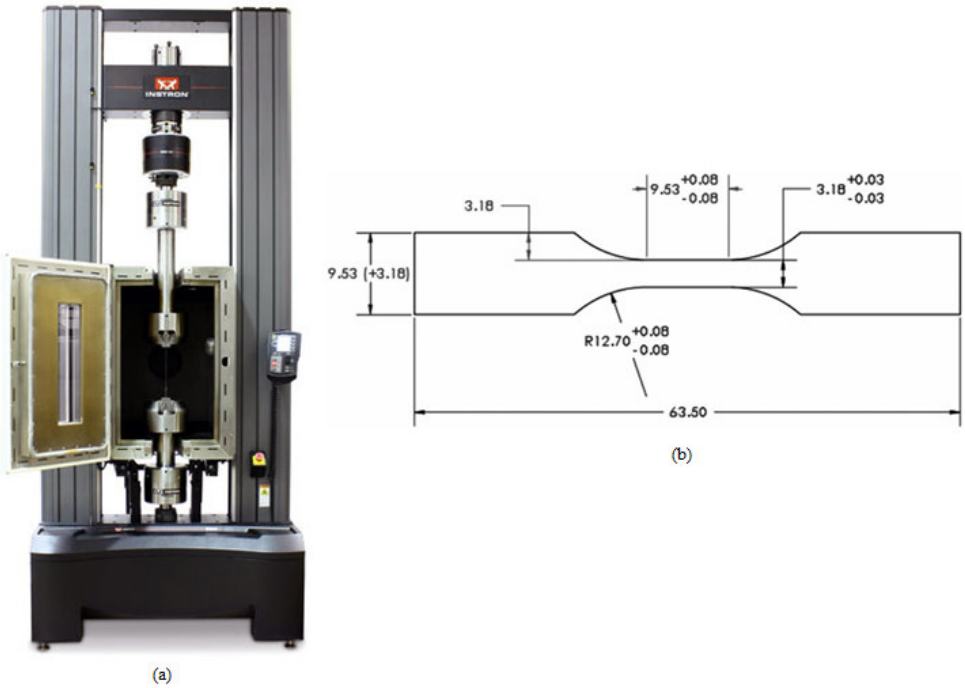

Figure 3: Tensile testing: UTM with temperature controlled chamber and (b) shape and dimensions of tensile specimen.

AA3003 alloy/TiN composites were fabricated by the stir casting process and low pressure casting technique with argon gas at 3.0 bar. The composite samples were give solution treatment and cold rolled to the predefined size of tensile specimens. The heat-treated samples were machined to get flat-rectangular specimens (figure 3) for the tensile tests. The tensile specimens were placed in the grips of a Universal Test Machine (UTM) with temperature controlled chamber at a specified grip separation and pulled until failure. The test speed was 2 mm/min. A strain gauge was used to determine elongation. In the current work, a cubical representative volume element (RVE) was implemented to analyze the tensile behavior AA3003/TiN nanoparticle composites at two (10% and 30%) volume fractions of TiN and at different temperatures. The large strain PLANE183 element was used in the matrix in all the models. In order to model the adhesion between the matrix and the particle, a CONTACT 172 element was used.

3. RESULTS AND DISCUSSION

The optical micrograph as shown in figure 4 reveals uniform distribution of TiN particles in AA3003 alloy matrix.

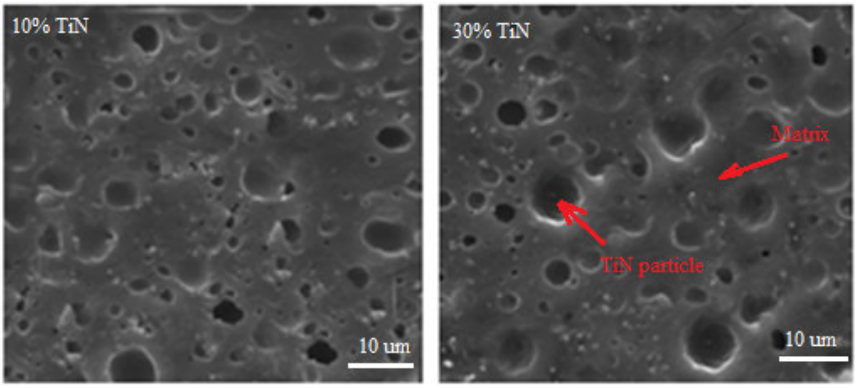

Figure 4: Microstructure showing distribution of TiN nanoparticles in AA3003 alloy matrix.

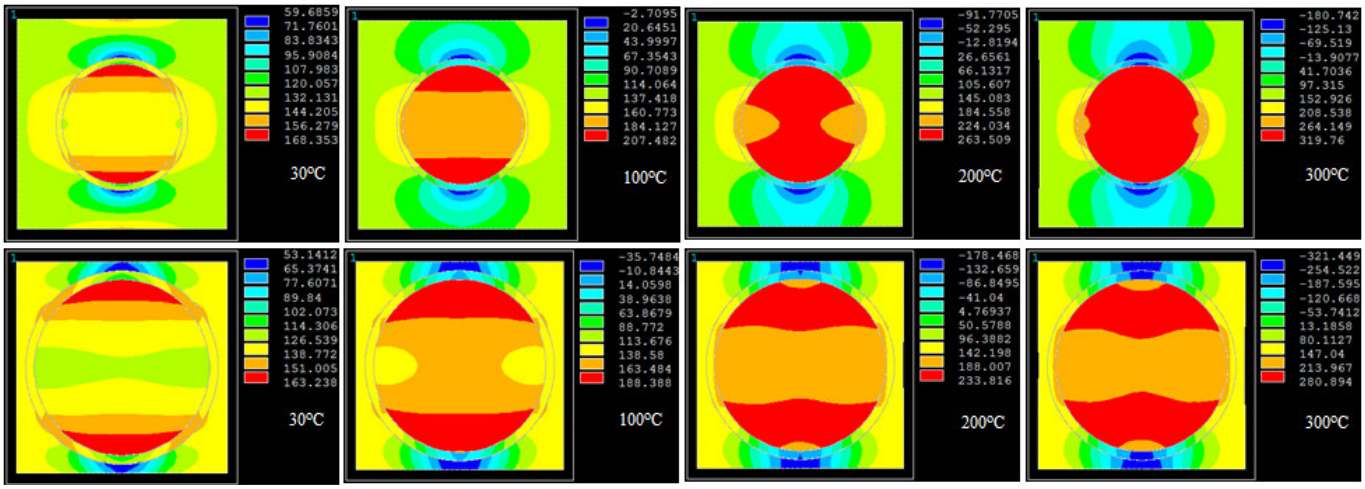

Figure 5: FEA results of tensile stress induced along load direction in the composites comprising of: (a) 10% TiN and (b) 30% TiN.

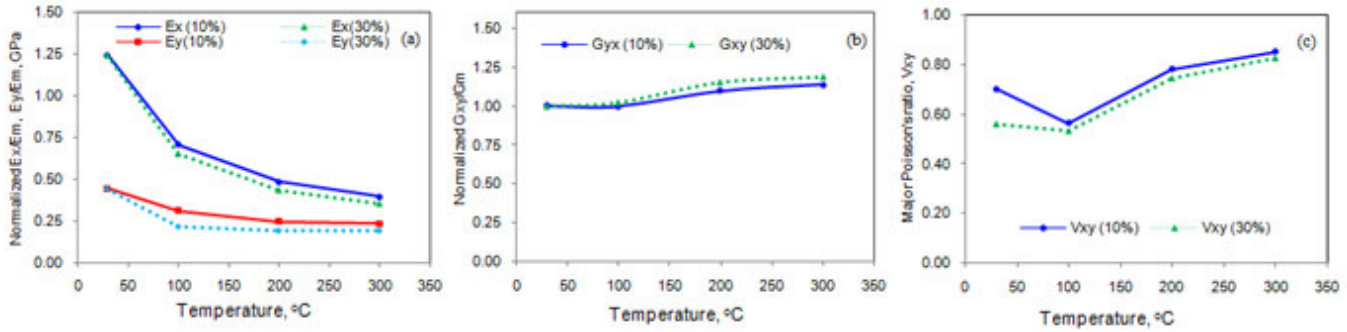

Figure 6: Effect of temperature on stiffness of AA3003/TiN composites.

3.1 Thermo-Mechanical Behavior

Figure 5 represents the tensile stresses induced in the AA3003/TiN composites along the load direction. The tensile stress increases with increase of temperature and it decreases with increase of volume fraction of AA3003/TiN in AA3003 alloy matrix. This is due to softening of the composite with increase of temperature. The normalized elastic modulus is shown in figure 6a. The elastic modulus is normalized with the elastic modulus of AA3003 alloy. The stiffness of the composites decreases with increase of temperature. The stiffness of AA3003 alloy/10%TiN composites is higher than that of AA3003 alloy/30%TiN composites with regard to increase of temperature. The normalized stiffness along the normal direction is lower

than that along the load direction. The normalized shear modulus increases with volume fraction of TiN (figure 6b). Initially, the major Poisson's ratio decrease from 30°C to 100°C and later on it increases with temperature from 100°C to 300°C (figure 6c).

3.2 Fracture Analysis

If the particle deforms in an elastic manner (according to Hooke's law) then,

$$\tau = \frac{n}{2}\sigma_p \quad (1)$$

where σ_p is the particle stress. If particle fracture occurs when the stress in the particle reaches its ultimate tensile strength, $\sigma_{p,uts}$, then setting the boundary condition at

$$\sigma_p = \sigma_{p,\,uts} \quad (2)$$

The relationship between the strength of the particle and the interfacial shear stress is such that if

$$\sigma_{P,uts} < \frac{2\tau}{n} \quad (3)$$

Then the particle will fracture. From the figure 7b, it is observed that the TiN nanoparticle was not fractured as the condition in Eq. (3) is not satisfied below 200°C, but the particle has occurred above 200°C. This is due to CTE mismatch between TiN nanoparticles and AA3003 alloy matrix. For the interfacial debonding/yielding to occur, the interfacial shear stress reaches its shear strength:

$$\tau = \tau_{max} \quad (4)$$

For particle/matrix interfacial debonding can occur if the following condition is satisfied:

$$\tau_{max} < \frac{n\sigma_p}{2} \quad (5)$$

It is observed from figure 7a that the interfacial debonding occurs between TiN nanoparticle and AA3003 alloy matrix as the condition in Eq.(5) is satisfied. The debonding phenomenon is high in the composites comprising of 30% TiN.

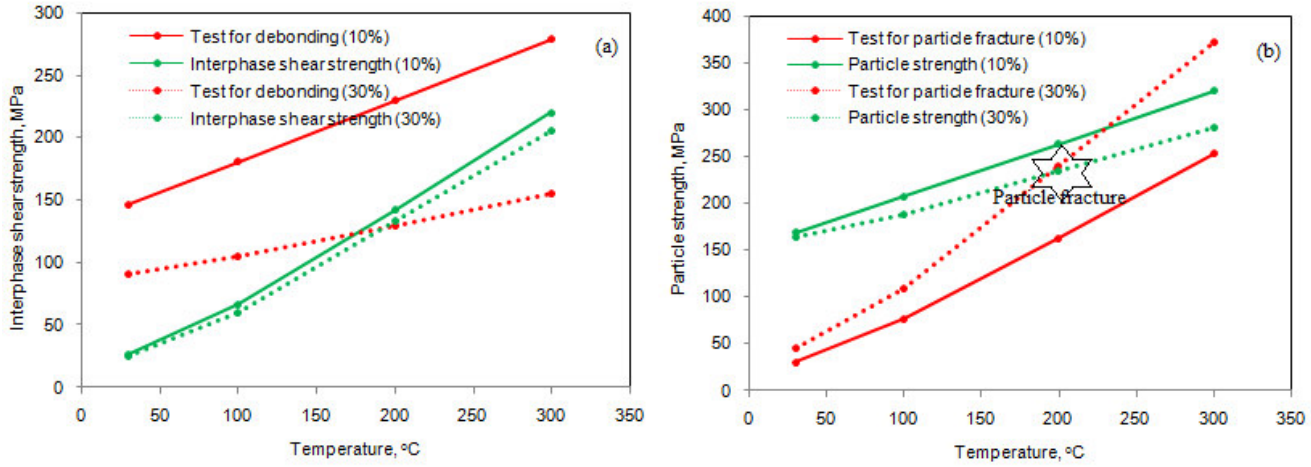

Figure 7: Criterion for interfacial debonding (a) and for particle fracture (b).

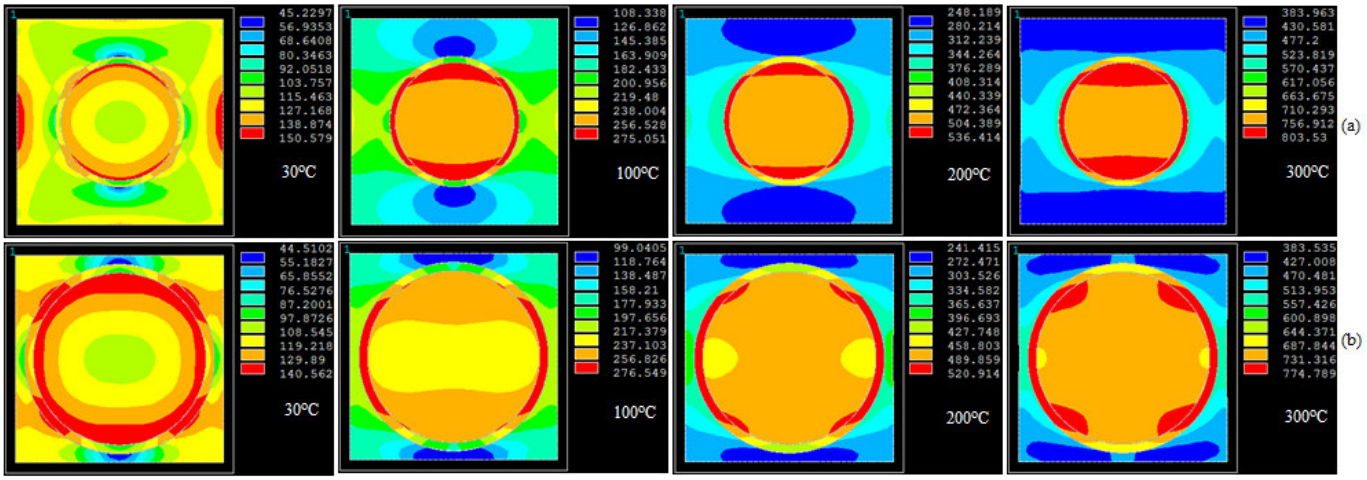

Figure 8: Images of von Mises stresses obtained from FEA: (a) AA3003/10% TiN and (b) AA3003/30% TiN composites.

The von Mises stress induced at the interface are higher than that induced in the nanoparticle (figure 8). Hence, the interfacial debonding was occurred between the particle and the matrix. The microstructure shown in figure 9 confirms the occurrence of interfacial debonding in the composites. The debris of the fractured interphase is also seen in the microstructure. The interfacial debonding increases with increase of temperature.

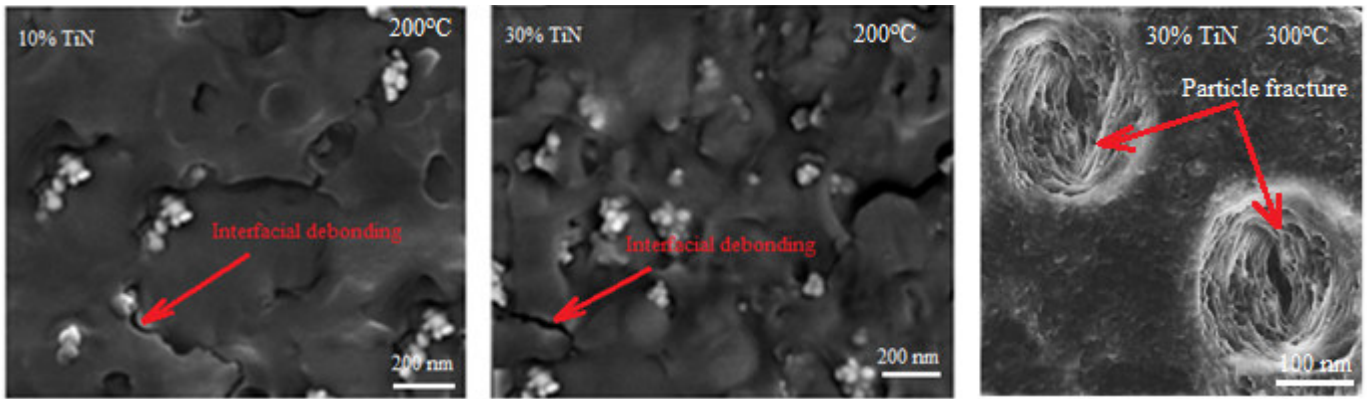

Figure 9: Microstructure showing the interfacial debonding and particle fracture in AA3003 alloy/TiN composites.

4. CONCLUSION

The microstructure of AA3003 alloy/TiN composites reveals the uniform distribution of TiN nanoparticles in the matrix. The shear stress is high at the interface resulting to interfacial debonding in AA3003/TiN composites. TiN particle fractures above 200°C. The microstructure obtained from the experimental samples confirms the fracture of interphase between the TiN particles and AA3003 alloy matrix and the fracture of TiN particle above 200°C of thermal loading.

REFERENCES

1. A. Agbossou, J. Pastor, Thermal Stresses and Thermal Expansion Coefficients of n-Layered Fiber-Reinforced Composites, Composite Science & Technology, 57, 1997, pp. 249-260.
2. A. Chennakesava Reddy, Effect of Particle Loading on Microealstic Behavior and interfacial Tractions of Boron Carbide/AA4015 Alloy Metal Matrix Composites, 1st International Conference on Composite Materials and Characterization, Bangalore, March 1997, pp. 176-179.
3. A. Chennakesava Reddy, Reckoning of Micro-stresses and interfacial Tractions in Titanium Boride/AA2024 Alloy Metal Matrix Composites, 1st International Conference on Composite Materials and Characterization, Bangalore, March 1997, pp. 195-197.
4. A. Chennakesava Reddy, Evaluation of Debonding and Dislocation Occurrences in Rhombus Silicon Nitride Particulate/AA4015 Alloy Metal Matrix Composites, 1st National Conference on Modern Materials and Manufacturing, Pune, India, 19-20 December 1997, pp. 278-282,.
5. A. Chennakesava Reddy, Interfacial Debonding Analysis in Terms of Interfacial Tractions for Titanium Boride/AA3003 Alloy Metal Matrix Composites, 1st National Conference on Modern Materials and Manufacturing , Pune, 19-20 December, 1997.
6. A. Chennakesava Reddy, Assessment of Debonding and Particulate Fracture Occurrences in Circular Silicon Nitride Particulate/AA5050 Alloy Metal Matrix Composites , National Conference on Materials and Manufacturing Processes, Hyderabad, India, 27-28 February 1998, pp. 104-109.
7. A. Chennakesava Reddy, Local Stress Differential for Particulate Fracture in AA2024/Titanium Carbide Nanoparticulate Metal Matrix Composites, National Conference on Materials and Manufacturing Processes, Hyderabad, India, 27-28 February 1998, pp. 127-131.
8. A. Chennakesava Reddy, Micromechanical Modelling of Interfacial Debonding in AA1100/Graphite Nanoparticulate Reinforced Metal Matrix Composites, 2nd International Conference on Composite Materials and Characterization, Nagpur, India, 9-10 April 1999, pp. 249-253.
9. A. Chennakesava Reddy, Cohesive Zone Finite Element Analysis to Envisage Interface Debonding in AA7020/Titanium Oxide Nanoparticulate Metal Matrix Composites, 2nd International Conference on Composite Materials and Characterization, Nagpur, India, 9-10 April 1999, pp. 204-209.

10. B. Kotiveera Chari, A. Chennakesava Reddy, Debonding Microprocess and interfacial strength in ZrC Nanoparticle-Filled AA1100 Alloy Matrix Composites using RVE approach, 2nd National Conference on Materials and Manufacturing Processes, Hyderabad, India, 10-11 March 2000, pp. 104-109.
11. A. Chennakesava Reddy, Micromechanical and fracture behaviors of Ellipsoidal Graphite Reinforced AA2024 Alloy Matrix Composites, 2nd National Conference on Materials and Manufacturing Processes, Hyderabad, India, 10-11 March 2000, pp. 96-103.
12. S. Sundara Rajan, A. Chennakesava Reddy, Micromechanical Modeling of Interfacial Debonding in Silicon Dioxide/AA3003 Alloy Particle-Reinforced Metal Matrix Composites, 2nd National Conference on Materials and Manufacturing Processes, Hyderabad, India, 10-11 March 2000, pp. 110-115.
13. S. Sundara Rajan, A. Chennakesava Reddy, Role of Volume Fraction of Reinforcement on Interfacial Debonding and Matrix Fracture in Titanium Carbide/AA4015 Alloy Particle-Reinforced Metal Matrix Composites, 2nd National Conference on Materials and Manufacturing Processes, Hyderabad, India, 10-11 March 2000, 116-120.
14. A. Chennakesava Reddy, Constitutive Behavior of AA5050/MgO Metal Matrix Composites with Interface Debonding: the Finite Element Method for Uniaxial Tension, 2nd National Conference on Materials and Manufacturing Processes, Hyderabad, India, 10-11 March 2000, pp. 121-127.
15. B. Kotiveera Chari, A. Chennakesava Reddy, Interfacial Debonding of Boron Nitride Nanoparticle Reinforced 6061 Aluminum Alloy Matrix Composites, 2nd National Conference on Materials and Manufacturing Processes, Hyderabad, India, 10-11 March 2000, pp. 128-133.
16. P. M. Jebaraj, A. Chennakesava Reddy, Simulation and Microstructural Characterization of Zirconia/AA7020 Alloy Particle-Reinforced Metal Matrix Composites, 2nd National Conference on Materials and Manufacturing Processes, Hyderabad, India, 10-11 March 2000, pp. 134-140.
17. P. M. Jebaraj, A. Chennakesava Reddy, Continuum Micromechanical modeling for Interfacial Debonding of TiN/AA8090 Alloy Particulate Composites, 2nd National Conference on Materials and Manufacturing Processes, Hyderabad, India, 10-11 March 2000, pp. 141-145.
18. A. A. Gusev, Representative volume element size for elastic composites: A numerical study, Journal of the Mechanics and Physics of Solids, 45, 1997, pp. 1449 – 1459.